

# Class-F and Inverse Class-F Power Amplifier Loading Networks Design Based upon Transmission Zeros

Ramon A. Beltran, *IEEE Member*.

Skyworks Solutions Inc., 2427 W. Hillcrest Drive, Newbury Park, CA 91320, USA.

E-mail: ramon.beltran@skyworksinc.com

**Abstract**— In practical implementations, class-F amplification is achieved based upon the second and/or third harmonic control provided by the output matching network. This paper presents a design method based upon inserting finite-frequency transmission zeros to a lumped-element matching network at the harmonic frequencies of interest. A two-section impedance matching network is transformed to either a class- $F_{2,3}$  or inverse class- $F_{2,3}$  loading network. The manipulation of transistor parasitics is described using network transformations. The resultant loading networks serve as fundamental-frequency matching and harmonic tuning simultaneously while reducing the number of components and circuit size. The simulated results show the expected wave shaping and drain impedances. The prototype amplifiers achieve 81% and 79% efficiency for the class-F and inverse class-F, respectively, at 42.32 and 42.37 dBm output powers at 300-MHz fundamental-frequency.

**Index Terms**— Amplifier, class-F, efficiency.

## I. INTRODUCTION

Power amplifiers (PAs) efficiency is enhanced by operating the transistor in different classes. Class-F PAs offer high power capabilities and high efficiency with a limited number of controlled harmonics [1]. In an ideal class-F PA the efficiency is 100% and is achieved by using an infinite number of harmonics to yield square and half-wave sinusoid waveform shapes at device drain for the voltage and current respectively. Inverse wave shaping is regarded as inverse class-F.

Typically, only one or two harmonics are controlled at a time, the second and/or third-harmonic (i.e. class- $F_{2,3}$ ), with a maximum theoretical efficiency of 81.65% when using an ideal device and the required impedances at each harmonic and fundamental-frequency ( $f_0$ ) at “virtual drain” ( $Z_{VD}$ ) [1], Fig 1.

Class-F output network designs have been reported in the literature using transmission lines as harmonic resonators where electrical lengths are practical [2]. Also, the classic class-F PA design has addressed output networks built based upon lumped-element resonators to peak one harmonic frequency and a shunt connected tank circuit tuned at  $f_0$  [3], [4]. However, when a real device is used, parasitics act against this design methodology.

In addition, the conventional approach requires harmonic tuning and a separate  $f_0$  matching network [3]. The following sections of this paper describe a design technique which encompasses harmonic control and  $f_0$  matching simultaneously as well as device parasitics manipulation for class-F PAs.

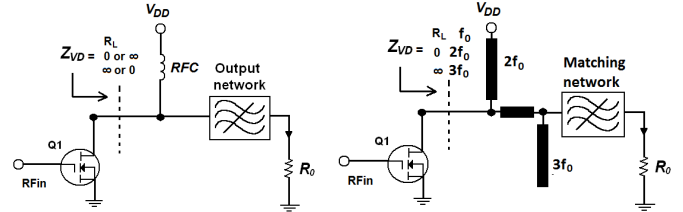


Fig. 1. Ideal class-F (right) and class- $F_{2,3}$  PA (left).

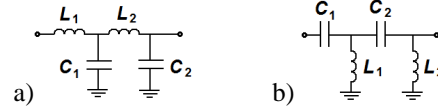


Fig. 2. Networks with Zero Transmission at  $\infty$  (a) and DC (b).

The loading network is derived from a two-section low-pass matching network with transmission zeros placed at the harmonic frequencies.

Network designed by transmission zeros is widely used in RF filter design and allows practical implementations with fewer components reducing insertion loss and achieving even more attenuation at the stop-band compared to those filters designed using cookbook methods [5], [6].

## II. CLASS-F PA OUTPUT NETWORKS DESIGNED BY TRANSMISSION ZEROS

A transmission zero (TZ) can be defined as an open or short circuit for three different cases; at DC, infinity and at a finite-frequency. In addition, it can be represented by a capacitor, an inductor and a resonator, respectively. For a ladder network, it is essential that the inductors and capacitors alternate so there is zero transmission at an infinite frequency for a low-pass network and zero transmission at DC for a high-pass network [5], Fig. 2. However, for a class-F PA loading networks with finite-frequency TZs at the harmonic frequencies are desired.

Since a two-section low-pass ladder network has TZs only at DC and infinity it could not be used to zero (notch) any frequency between DC and infinity. Therefore, it requires TZs at finite frequencies. I.e., for a two-harmonic controlled class- $F_{2,3}$  PA, two finite-frequency TZs are required, one at  $2f_0$  and the other at  $3f_0$ . This can be accomplished by embedding harmonic resonators into the low-pass network as shown in Fig. 3. Notice that the  $f_0$  equivalent circuit is a ladder LCLC network.

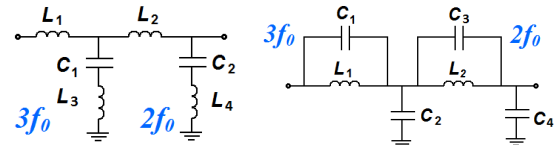


Fig. 3. Fine-frequency TZs low-pass networks.

### A. Loading Network for Class- $F_{2,3}$ PAs

Class- $F_{2,3}$  operation requires an open circuit at  $3f_0$  and a short circuit at  $2f_0$  so that the drain voltage waveform is shaped towards a square wave whereas the drain current is shaped such that it resembles a half-wave sinusoidal. A two-section low-pass network is converted to a class- $F_{2,3}$  PA loading network by placing TZs at the controlled harmonic frequencies. However, the network must create the right impedance at the device drain at  $f_0$ ,  $2f_0$  and  $3f_0$  taking into account transistor parasitics  $C_{DS}$  and  $L_{DS}$ , Fig. 4.

In Fig. 4 a network topology with two transmission zeros at finite frequencies is shown for a class- $F_{2,3}$  PA. This uses a shunt-connected series L-C resonators tuned at  $2f_0$  and  $3f_0$ .

The design procedure starts with  $3f_0$  control by computing the  $L_1$  inductor value which is a function of the estimated parasitic shunt capacitance  $C_{DS}$  and lead inductance  $L_{DS}$ . Since the  $3f_0$  resonator ( $C_1$  and  $L_3$ ) creates a short circuit at  $3f_0$  the combination of  $L_{DS}$  and  $L_1$  shunts  $C_{DS}$  as shown in the equivalent circuit of Fig. 5. This equivalent circuit resonates at  $3f_0$  producing an open circuit at  $Z_{VD}$ .  $L_1$  value can be computed from:  $L_1 = \{1/(C_{DS} \cdot (2\pi \cdot 3f_0)^2)\} - L_{DS}$ .

At the second harmonic, the  $3f_0$  resonator behaves as a shunt capacitor ( $C_1'$  in Fig. 6) and the  $2f_0$  resonator produces a short circuit. Judicious selection of  $C_1'$  and  $L_2$  yields to a short circuit at  $Z_{VD}$ , Fig. 6. Choosing  $L_2$  is not trivial since it plays an important role for the  $f_0$  matching. Therefore,  $L_2$  value selection must take into account  $C_1'$  and the impedance at node A in Fig. 6 for  $f_0$  matching. A numerical solution or computer optimization could be used.

### B. Loading Network for Inverse Class- $F_{2,3}$ PAs

In an inverse class- $F_{2,3}$   $3f_0$  short and  $2f_0$  open are required. The drain voltage waveform is shaped towards a half-wave sinusoidal whereas the drain current is shaped such that it resembles a square wave.

In analogy to the class- $F_{2,3}$ , a two-section low-pass matching network is converted to an inverse class- $F_{2,3}$  PA loading network by placing TZs at the controlled harmonic frequencies. Again, the network must create the right impedance at device drain at  $f_0$ ,  $2f_0$  and  $3f_0$  taking into account transistor parasitics. For the inverse class- $F_{2,3}$  the TZs are placed by adding shunt capacitors in parallel with the series inductors as shown in Fig. 4.

At  $3f_0$  the device drain is presented with a short circuit which is implemented via a resonator created by  $L_{DS}$ ,  $L_1$  and  $C_1$  in Fig. 4 since the series connected tank circuit formed by  $C_2$  and  $L_2$  yields to an open circuit as shown in Fig. 5. The addition of  $L_1$  inductor allows tuning flexibility; otherwise  $C_1$  would be a very large value capacitor since  $L_{DS}$  inductance is too low in order to resonate at  $3f_0$  in the VHF and lower UHF frequency bands.

At  $2f_0$ , the  $3f_0$  resonator behaves as a series inductor ( $L_2'$  in Fig. 6) and the  $2f_0$  resonator produces an open circuit. Judicious selection of  $L_2'$ ,  $C_1$  and  $C_3$  yields an open circuit at  $Z_{VD}$ , Fig. 6. Again, choosing  $L_2'$ ,  $C_1$  and  $C_3$  is not trivial since they play an important role for  $f_0$  matching.

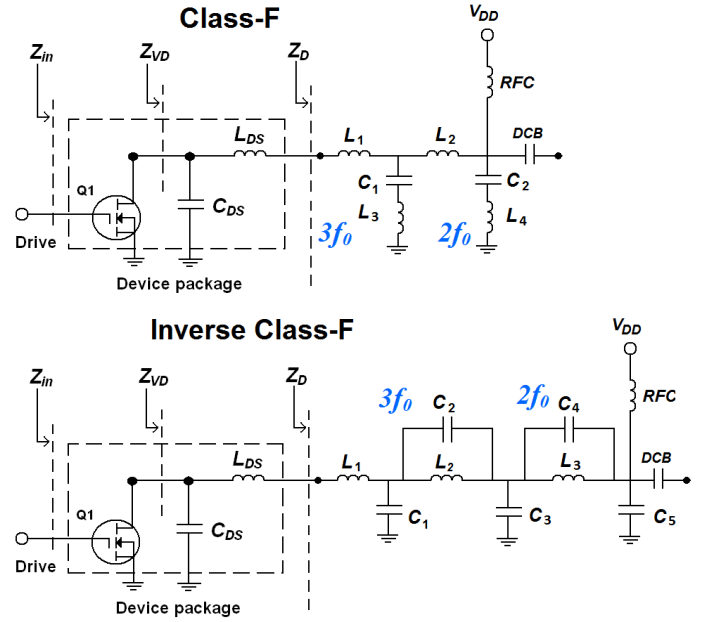


Fig. 4. Class- $F_{2,3}$  PA schematics.

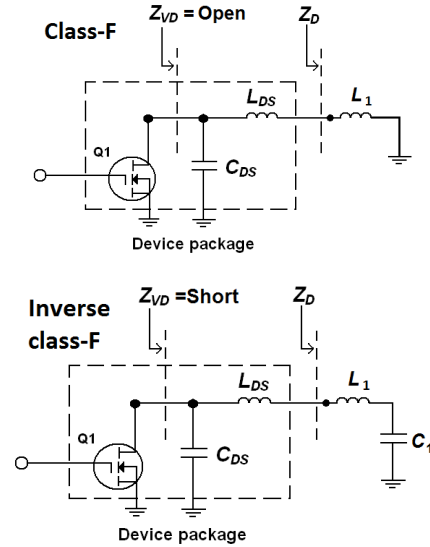


Fig. 5.  $3f_0$  class- $F_{2,3}$  PA equivalent circuits.

### C. Fundamental-frequency Matching

The  $f_0$  equivalent circuits look like LC ladder networks for both, class-F and inverse class-F and they present the required impedance at  $Z_{VD}$ , Fig. 7. The  $2f_0$  resonator represents a capacitive susceptance that can be chosen according to what is required for the  $f_0$  matching.

Once the component values are found to satisfy the three conditions:  $f_0$ ,  $2f_0$  and  $3f_0$  impedances presented at  $Z_{VD}$ , the transmission characteristics resemble those of a low-pass network with two TZs at finite frequencies.

For a class- $F_{2,3}$  and inverse class- $F_{2,3}$  PA designed to operate at  $f_0=300$ -MHz the frequency responses of the output networks from Fig. 4 are shown in Fig. 8 and 9, respectively. The finite-frequency TZs appear at the harmonic frequencies and the impedances seen at the device drain are plotted on the Smith chart showing an open/short circuit at  $3f_0$  (900-MHz), a

short/open circuit at  $2f_0$  (600-MHz) for class-F and inverse class-F, respectively, and a  $f_0$  load impedance of 29.8-Ohms.

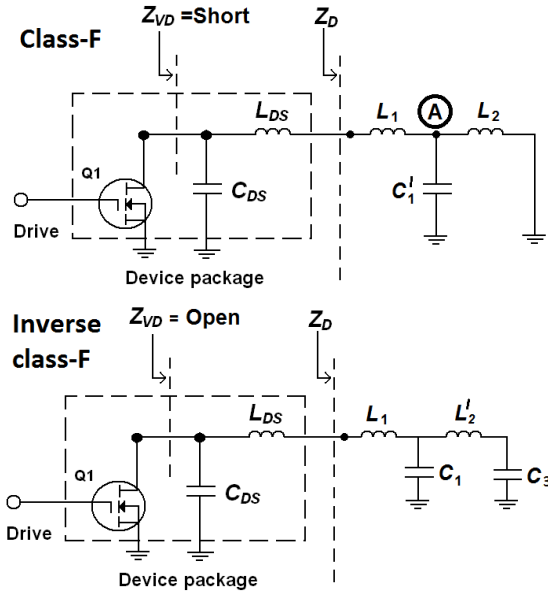


Fig. 6.  $2f_0$  class-F<sub>2,3</sub> PA equivalent circuits.

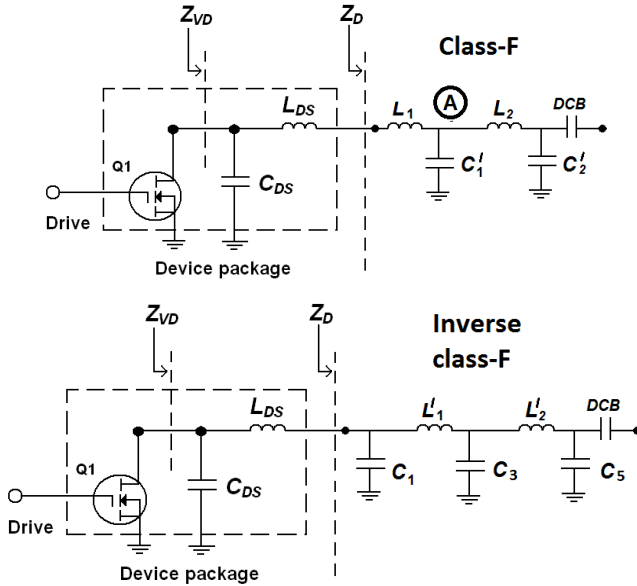


Fig. 7.  $f_0$  class-F<sub>2,3</sub> PA equivalent circuits.

### III. CLASS-F POWER AMPLIFIER DESIGN

In a class-F<sub>2,3</sub> PA the effects of the controlled harmonics in a given waveform are manifested in waveform factors and [1] relate the DC components to the  $f_0$  components and peak drain voltage and current.

#### A. Class-F<sub>2,3</sub> PA Design

The waveform coefficient values for a class-F<sub>2,3</sub> are [1]:  $\gamma_V=1.1547$ ,  $\delta_V=2$ ,  $\gamma_I=1.414$ ,  $\delta_V=2$  and  $\delta_I=2.914$ . Since  $\delta_V=2$  the standard supply voltage of 28 V produces a maximum drain voltage  $V_{Dmax} = \delta_V \cdot V_{DD} = 56$  V. Allowance for the on-state

resistance of 0.35-Ohms gives an effective supply voltage of  $V_{eff} = V_{DD} / (R_L / (R_L + 1.365 R_{ON})) = 27.56$  V and an output RF voltage of  $V_{om} = \gamma_V \cdot V_{eff} = 31.82$  V.

The  $f_0$  resistance is then selected to be 29.8-Ohms which gives 17 W of output power,  $P_{out} = V_{om}^2 / (2 \cdot R_L)$ .

The drain current is then;  $I_{DC} = \gamma_V V_{eff} / (\gamma_I R_L) = 0.775$  A which leads to a maximum DC current of  $I_{Dmax} = \delta_I \cdot I_{DC} = 2.2$  A being a safe margin for a 6-A  $I_{dsat}$  device such as the Polyfet GP2001. The output RF current is computed as  $I_{om} = \gamma_I \cdot I_{DC} = 1.068$  A. Subsequently, the DC input power can be computed as:  $P_{DC} = V_{DD} \cdot I_{DC} = 21.14$  W for a drain efficiency of 80.41 %.

The loading network previously described produces the required load impedance at  $Z_{VD}$  for a class-F<sub>2,3</sub> amplifier. This is confirmed by a harmonic balance simulation using a generic FET model which includes parasitics  $C_{DS}$  (8.5 pF) and  $L_{DS}$  (0.4 nH). Fig. 8 shows the normalized drain impedances presented at  $Z_{VD}$ , at  $f_0$  (29.8-Ω),  $2f_0$  and  $3f_0$ , for a class-F PA. The representative waveforms are depicted in Fig 10.

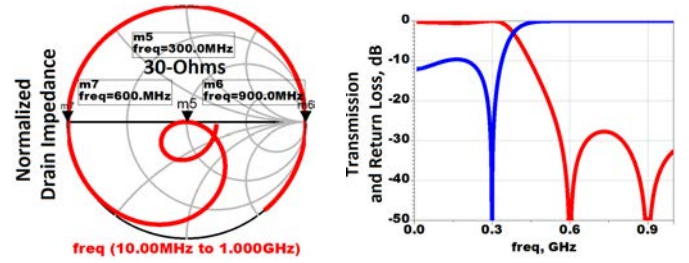


Fig. 8. Drain impedances and TZ at  $2f_0$  and  $3f_0$  for class-F.

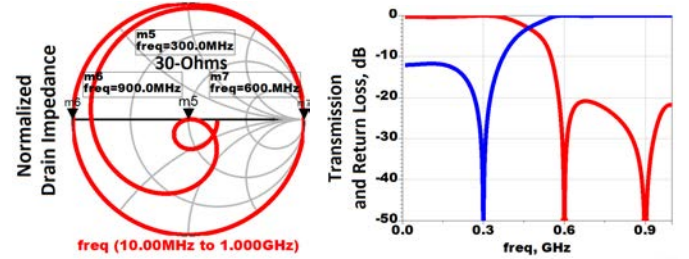


Fig. 9. Drain impedances and TZ at  $2f_0$  and  $3f_0$  for inverse class-F.

#### B. Inverse class-F<sub>2,3</sub> PA Design

An inverse class-F<sub>2,3</sub> PA requires harmonic impedances opposite to that of a class-F amplifier. The design process is similar to that of the class-F<sub>2,3</sub> described previously.

The inverse class-F<sub>2,3</sub> output network previously described produces the impedances required for this class of amplification including device parasitic. The same load impedance at  $f_0$  and supply voltage is used as for the class-F<sub>2,3</sub> amplifier. The impedances at  $Z_{VD}$  are as expected, Fig. 9.

Fig. 10 shows the drain waveforms that resemble those of the inverse class-F PA.

### IV. CLASS-F PAS IMPLEMENTATION

The amplifiers are input matched for  $f_0=300$ -MHz using an LCLC network and 10-Ohms stabilization resistances, Fig.11. The output networks use high-Q high self-resonance frequency trimmer capacitors and high-Q air core inductors.



The implementation is straightforward following schematics from Fig. 4. Notice that for the inverse class-F  $C_2$  and  $C_4$  in Fig. 4 are high-Q ceramic capacitors.

Tuning the output networks require alignment of the  $2f_0$  and  $3f_0$  resonators to achieve frequency responses similar to those shown in Fig. 8 and 9 with the device parasitics included. Nonetheless, a direct measurement of the output network not including device parasitics could be performed in order to verify the two TZs at the harmonic frequencies. Then, tuning for the expected peak output power is the key performance indicator for the targeted  $f_0$  impedance at  $Z_{VD}$ . Consequently, peak output power, harmonic suppression and DC drain current are monitored when tuning the output networks.

The measured efficiencies achieve 81% and 79% for the class-F and inverse class-F respectively. The output power for the class-F PA is 42.32 dBm, whereas the inverse class-F output power is 42.37 dBm as shown in Fig. 12.

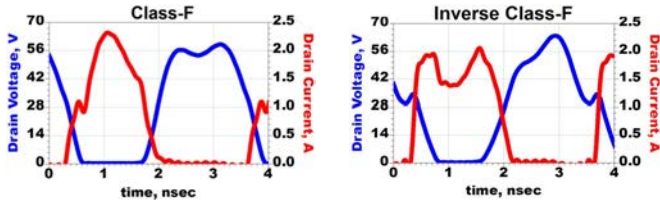


Fig. 10. Simulated class-F<sub>2,3</sub> waveforms.

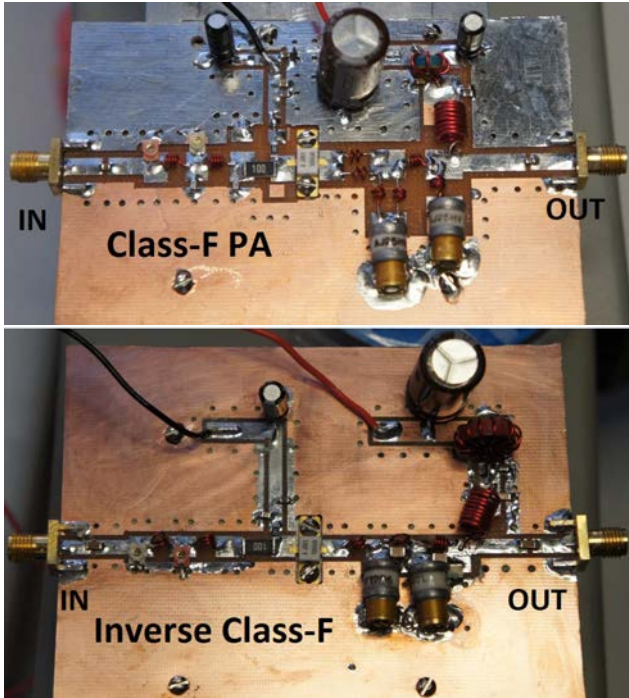


Fig. 11. Class-F<sub>2,3</sub> PA prototypes.

## V. CONCLUSIONS

A design method for class-F PAs output networks is presented. The combination of filter theory and network transformations allows the design of compact PA output networks providing harmonic tuning and impedance matching simultaneously yielding high efficiency PAs.

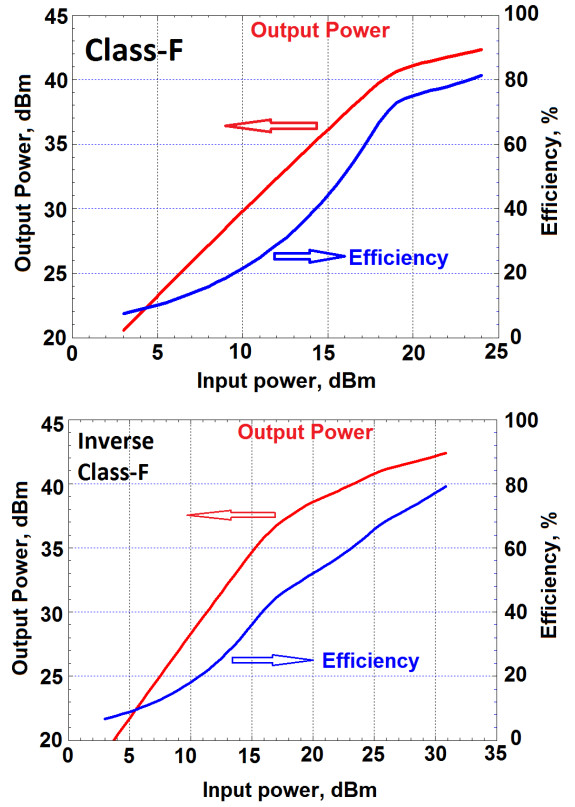


Fig. 12. Measured output power and efficiency of the class-F<sub>2,3</sub> PAs.

## VI. ACKNOWLEDGMENTS

The author wishes to thank Mr. Jerome Citrolo and Mr. Marcos Cervantes from PolyFet RF Devices for providing the GP2001 GaN FETs samples used for the experimental work and discussing the amplifiers implementation.

## REFERENCES

- [1] F. H. Raab, "Maximum Efficiency and Output of Class-F Power Amplifiers". IEEE Transactions on Microwave Theory and Techniques, Vol. 49, No. 6, June 2001.
- [2] A. V. Grebennikov, "Load network design for high-efficiency class-F power amplifiers," IEEE MTT-S Int. Microwave Symposium. Dig., vol. 2, Boston, MA, June 13–15, 2000, pp. 771–774.
- [3] C. Trask, "Class-F Amplifier Loading Networks: A Unified Design Approach". IEEE MTT-S Int. Microwave Symposium. Dig. Anaheim, CA, June 13–18, 1999.
- [4] P. Colantonio, F. Giannini, G. Leuzzi, E. Limiti, "On the Class0-F Power Amplifier Design," *Int. Journal on RF and Microwave Computer-Aided Engineering*, vol. 9, no. 2, pp. 129–149, March 1999.
- [5] Randall Rhea, "HF Filter design and computer simulation", Noble Publishing. 1994.
- [6] H. J. Orchard and Gabor C. Temes. "Filter Design Using Transformed Variables". IEEE Transactions on Circuit Theory, Vol. C-T 15, No. 4, December 1968.